Frontiers of Architectural Research 12 (2023) 788–802

Available online at www.sciencedirect.com

ScienceDirect

journal homepage: www.keaipublishing.com/foar

RESEARCH ARTICLE

Detection of deteriorations in cultural structures created by carving into low-strength rocks by the non-destructive test (NDT) method

Fatma Özer [a], Mehmet Söylemez [b,*], İsmail İnce [c], Osman Günaydin [b]

[a] *Graduate Education Institute, Adıyaman University, Adıyaman 02240, Turkey*
[b] *Faculty of Engineering, Department of Civil Engineering, Adıyaman University, Adıyaman 02240, Turkey*
[c] *Faculty of Engineering and Natural Sciences, Department of Geological Engineering, Konya Technical University, Konya 42079, Turkey*

Received 6 October 2022; received in revised form 18 March 2023; accepted 31 March 2023

KEYWORDS
Pyroclastic;
Kilistra ancient city;
Deterioration;
Non-destructive test;
Weak-strength rock

Abstract In the cultural stone heritage, progressive deteriorations develop over time with the effect of atmospheric processes. These deteriorations can reach to a significant degree that threaten the integrity of the monuments built from weak-strength rocks. In this study, it is aimed to determine the deteriorations caused by atmospheric processes on the monument surface in cultural heritage works built by carving into low-strength pyroclastic rocks by non-destructive tests (NDTs). To this end, two historic structures in the Kilistra Ancient City of Konya (Turkey) were selected. The index, strength, mineralogical and petrographic properties of the rocks, in which the monuments were carved, were first investigated. Then, contour scaling, crack, efflorescence and biodeterioration types were determined on the facades of the monuments. Later, NDT deterioration change maps were prepared based on the data obtained by performing the relative humidity, Schmidt hammer rebound (SHR), and P-wave velocity (*Vp*) measurements on the facades of the monuments. In the deterioration maps, it was determined that the SHR and *Vp* values of the rock were low in the capillary, infiltration, and crack zones with water penetration in the monuments built on low-strength pyroclastic rocks. However, deterioration was less in the regions with more limited water access according to zones.

* Corresponding author.
E-mail address: msoylemez@adiyaman.edu.tr (M. Söylemez).
Peer review under responsibility of Southeast University.

https://doi.org/10.1016/j.foar.2023.03.004

1. Introduction

The adventure of the use of rocks that are widely spread around human beings, starting from the ax as a defense and/or war tool, has evolved into a work of art sculpture. However, from past to present, rocks have remained as one of the main materials used in the construction of buildings for protection, living, and worship purposes. The cultural heritage created from rocks is directly or indirectly affected by atmospheric processes, which results in changes in their textural, physical, and strength properties (Fener and İnce, 2015; İnce et al., 2018). In line with the extension of the period of being affected by these processes, damages may reach alarming levels. The detection, identification, and evaluation of damage to building stones over time and measuring and classifying the amount of damage are among the measures for the effective and economical conservation of monumental works. Determining the amount of deterioration of the building stones of the monument and preparing deterioration maps for the monument are an innovative damage assessment method. Non-destructive tests (NDTs) have started to be used as an important method in determining the amount of deterioration of monuments (Fais et al., 2017).

While researchers initially investigated deteriorations in the monuments built from building stones using a single NDT method (Christaras, 1997; Christaras et al., 2015; Hatır, 2020; Jo and Lee, 2014; Mol and Preston, 2010), then deteriorations in the monuments were investigated using several NDT methods together (Bozdağ et al., 2020; Fais et al., 2017; Fort et al., 2013; Hatır et al., 2022; İnce et al., 2018; Kilic, 2015; Korkanç et al., 2019; Tosunlar et al., 2020; Valero et al., 2019; Wu et al., 2021) (Table 1). Christaras (1997) stated that the P-wave velocity can be used to determine the depth of the deterioration surface of the building blocks. Some researchers have reported that the P-wave velocity test results gathered from stone monuments can provide important information for the determination of deterioration and consolidation studies in these monuments (Christaras, 1997; Christaras et al., 2015; Hatır 2020). Jo and Lee (2014) presented that using infrared thermography, it is possible to quickly and quantitatively determine the deterioration zones and the relative degree of deterioration in monuments. Mol and Preston (2010) emphasized that the electrical resistivity tomography method could help to understand the water content and degradation process in monuments. Kilic (2015) used ground penetrating radar and infrared thermography in a historic masonry school to reveal significant cracks and other defects in various parts of the monument. Some other researchers declared that the interpretation of the deterioration map and NDT data together gives more accurate results (Bozdağ et al., 2020; Hatır et al., 2022; İnce et al., 2018; Tosunlar et al., 2018, 2020). Korkanç et al. (2019) expressed that the sulfation effect caused by air pollution can be determined by infrared thermography methods. Some researchers investigated deteriorations in the stone heritage carved into rock (limestone, sandstone, and andesite) using the NDT methods (İnce et al., 2020; Korkanç et al., 2018, 2021; Zhang et al., 2019) (Table 1). Korkanç et al. (2018) investigated the deterioration of the facades of a mosque carved into limestone using surface moisture, Schmidt hammer rebound (SHR) test, infrared thermography methods. İnce et al. (2020) studied the deterioration of the facades of a tomb carved into volcanic rock using P-wave velocity, surface and deep moisture methods. They stated that the development of biological colonization is common in areas with high humidity (superficial and deep) conditions. Korkanç et al. (2021) investigated the deterioration in rock relief using some NDT methods (ultrasonic velocity, surface moisture, SHR test infrared thermography).

However, deteriorations in monuments in pyroclastic rocks, which are sensitive to atmospheric processes and in which many cultural heritage works were built by carving, were not investigated using the NDT methods. To this end, the ancient city of Kilistra built by carving into pyroclastic rocks, the sensitivity of which to atmospheric processes was also emphasized by Bozdağ et al. (2016), during the Early-Late Byzantine period was chosen as the study area. In addition, Bozdağ (2022) emphasized that some parts of the ancient city had rockfalls associated with deterioration. For this purpose, the changes in the facades of two historic structures chosen in the ancient city of Kilistra were investigated using the NDT methods (P-wave velocity, Schmidt hammer, and surface moisture device). It is aimed to create bases for restoration projects so that these two monuments can be passed on to future generations.

2. Characteristics of the monuments studied in the ancient city of Kilistra

The ancient city of Kilistra is located in the Gökyurt neighborhood, 35 km southwest of Konya Province. The region consists of churches, chapels, houses, observation towers, cellars, graves, ancient roads, and water structures built by carving into pyroclastic rocks in 5 different locations during the Early Byzantine period (Fig. 1) (Mimiroğlu, 2005).

The first of the structures to be examined in the ancient city of Kilistra is the chapel dated between the 7th and 10th centuries. The chapel is located in the east-west direction and has a free cross plan, and there are apsis, naos, kose burial chamber, and entry sections (Fig. 2a; Table 2) (Özkan, 2001). The second structure is the rectory planned as a 2-storey regular rectangular geometric structure opposite the chapel (Fig. 2b and c; Table 2). Although the exact date of building of the rectory's is unknown, similar

Table 1 Studies in the literature to determining the deterioration of cultural monuments by means of NDT.

Form of construction	Monument	Rock type	Applied method	References
Built using building stones	Tomb, church	Marble, travertine	Ultrasonic velocity	Christaras (1997)
	Rock art	Different rock types	Electrical resistivity tomography	Mol and Preston (2010)
	Temple	Different rock types	Infrared thermography	Jo and Lee (2014)
	Church, street	Limestone	Ultrasonic velocity	Christaras et al., (2015)
	Mausoleum	Dacite	Ultrasonic velocity	Hatır (2020)
	Church, bridge	Several types of granite	Ultrasonic velocity, Schmidt hammer rebound test	Fort et al., (2013)
	School	Limestone	Ground penetrating radar, infrared thermography	Kilic (2015)
	Cathedra	Carbonate	Ultrasonic velocity, terrestrial laser scanner	Fais et al., (2017)
	Cistern	Limestone	Ultrasonic velocity, Schmidt hammer rebound test, humidity, infrared thermography	İnce et al., (2018)
	Bridge	Dacite	Surface moisture, Schmidt hammer rebound test	Tosunlar et al., (2018)
	Church	Andesite	Ultrasonic velocity, surface moisture, Schmidt hammer rebound test	Hatır et al., (2019)
	Madrasa	Marble, Pyroclastic	Portable XRF, infrared thermography	Korkanç et al., (2019)
	Church	Limestone	Infrared thermography, electrical resistance	Valore et al., (2019)
	Water monument	Dacite	Ultrasonic velocity, surface moisture, Schmidt hammer rebound test	Bozdağ et al., (2020)
	Mausoleum	Andesite	Ultrasonic velocity, surface moisture, Schmidt hammer rebound test	Tosunlar et al., (2020)
	Cultural artifacts	Limestone, Marble	Surface roughness, Schmidt hammer rebound test, shore hardness meter, infrared thermography, surface moisture	Wu et al., (2021)
Carved into rock	Stone mosque	Limestone	Surface moisture, Schmidt hammer rebound test, infrared thermography	Korkanç et al., (2018)
	Rock carved statue	Sandstone	Leeb hardness, ultrasonic velocity	Zhang et al., (2019)
	Rock tomb	Dacite	Surface moisture, deep moisture, ultrasonic velocity	İnce et al., (2020)
	Rock monument	Limestone	Ultrasonic velocity, surface moisture, Schmidt hammer rebound test, infrared thermography	Korkanç et al., (2021)
	Han	Different rock types	Infrared thermography, deep moisture	Hatır et al., (2022)

architectural techniques and features suggest that it was erected around the same time as the chapel (Mimiroğlu, 2005). The access to the second floor of this structure is provided through a space with a circular section on the first floor (Table 2). On the second floor, there is a bed terrace carved from the parent rock (Table 2).

3. Climate and temperature

The climate (precipitation, temperature, average sunshine duration, dominating wind direction, and wind speed) of the location must be understood in order to comprehend the climatic processes that cause the destruction of cultural artifacts. The ancient city of Kilistra is located in the province of Konya, in the Central Anatolian region of Turkey. The GPS coordinates of the chapel and rectory monuments in the ancient city of Kilistra are 37.66589 N; 32.21380 E and 37.66591 N; 32.21385 E, respectively. For this purpose, regional meteorological data were utilized to investigate the impact of atmospheric occurrences on the ancient city of Kilistra. The climate of the region where the monuments are located is terrestrial. Summers are hot and

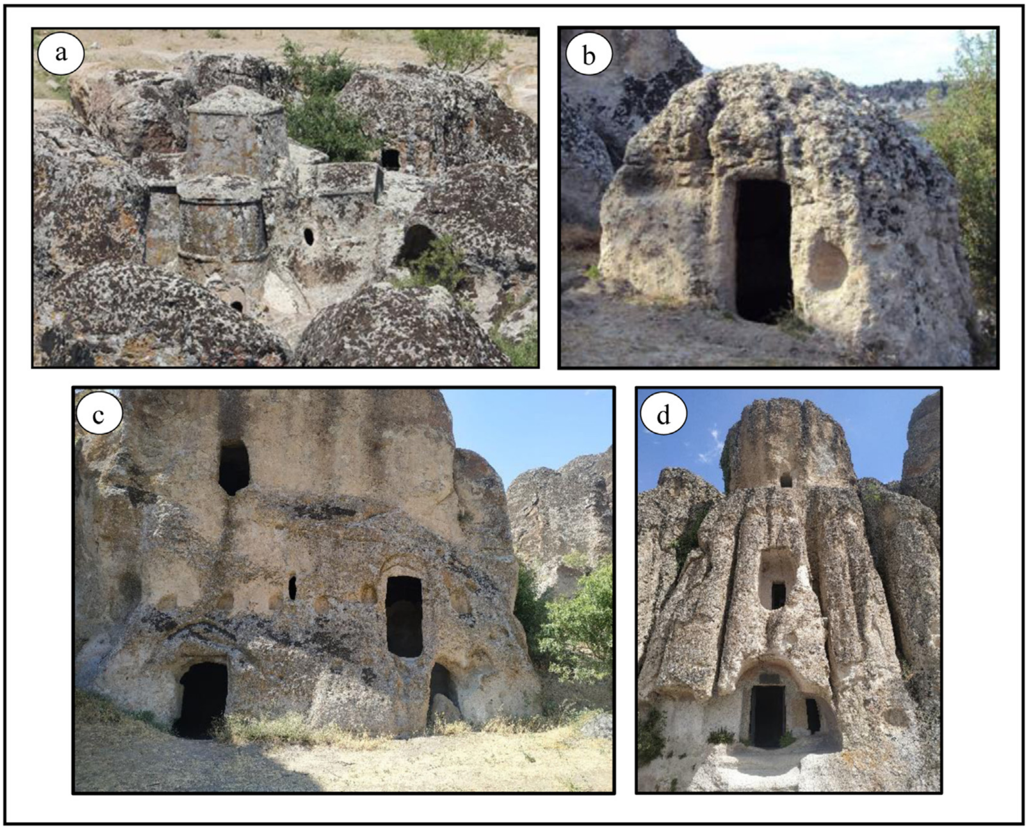

Fig. 1 Structures built by carving into pyroclastic rocks in the ancient city of Kilistra: a) top view of the cross church, b) house, c) complex structure (house, store and hayloft), d) monastery.

dry in a continental environment, while winters are cold and wet (Table 3) (MGM 2022). From 1929 to 2021, the average precipitation is 329.4 mm and the average temperature is 11.7 °C (MGM 2022). According to the long-term average, the wettest months are December (43.2 mm), May (43.1 mm), and January (38.1 mm); July (7.5 mm) and August (6.4 mm) have the least precipitation (Table 3) (MGM 2022). July (11.8 h) and August (11.4 h) have the region's longest average sunlight duration (MGM 2022). According to the average annual precipitation and average annual temperature figures indicated by Fookes et al. (1971), the region's deterioration class is very slight weathering. The major wind direction in the region is north (Fig. 2c).

4. Materials and methods

The experimental studies within the scope of this research were conducted in two stages, *in situ* and laboratory. For the laboratory study, three blocks of 20 × 30 × 30 cm^3 were collected from the region where the pyroclastic rocks, in which the ancient city of Kilistra was carved, outcropped. The core samples with a diameter of NX (a diameter of 54 mm) according to the ISRM (2007) were prepared to determine the physical (porosity, dry density, and P-wave velocity) and strength (uniaxial compressive strength and SHR) properties of the samples. While the porosity and dry density values of the rocks were determined according to the standards specified in the ISRM (2007), the P-wave velocity values for saturated and dry conditions were determined by considering the standards recommended in the ASTM E494 (2010). Porosity values of the rocks were determined by applying saturation and caliper procedures (ISRM 2007). To determine the dry density of rocks in which the structures were carved, the volume of the rock samples was first calculated by averaging several caliper readings. The dry density of the samples was then calculated as the mass of the unit volume of the rock sample. P-wave velocity test was applied to determine the change in the internal structure of the rock in which the monument was carved. The P-wave velocity of the rocks was measured *in situ* and in the laboratory by direct transmission using a device that measures the propagation time of ultrasound pulses with an accuracy of 0.1 μs. The capillary water absorption test was conducted in accordance with the methods proposed by the standard TS EN-1925 (2000). The amount of water absorption per unit area (g/m^2) of the samples immersed in water was determined at regular time intervals (1, 3, 5, 10, 15, 30, 60, 480, 1440 min) in accordance with the standards. The measurements were completed when the difference between two consecutive measurements were less than 1% of the water absorbed by the samples. Then, the graphs of the changes in the measurements were prepared according to the square root of the measurement time ($t^{1/2}$). The slope of these graphs was defined as the capillary water absorption (C) value of the sample. The UCS tests were applied on core samples (ISRM, 2007). The stress within the limits of 1.0 ± 0.5 MPa/s was performed. The average of

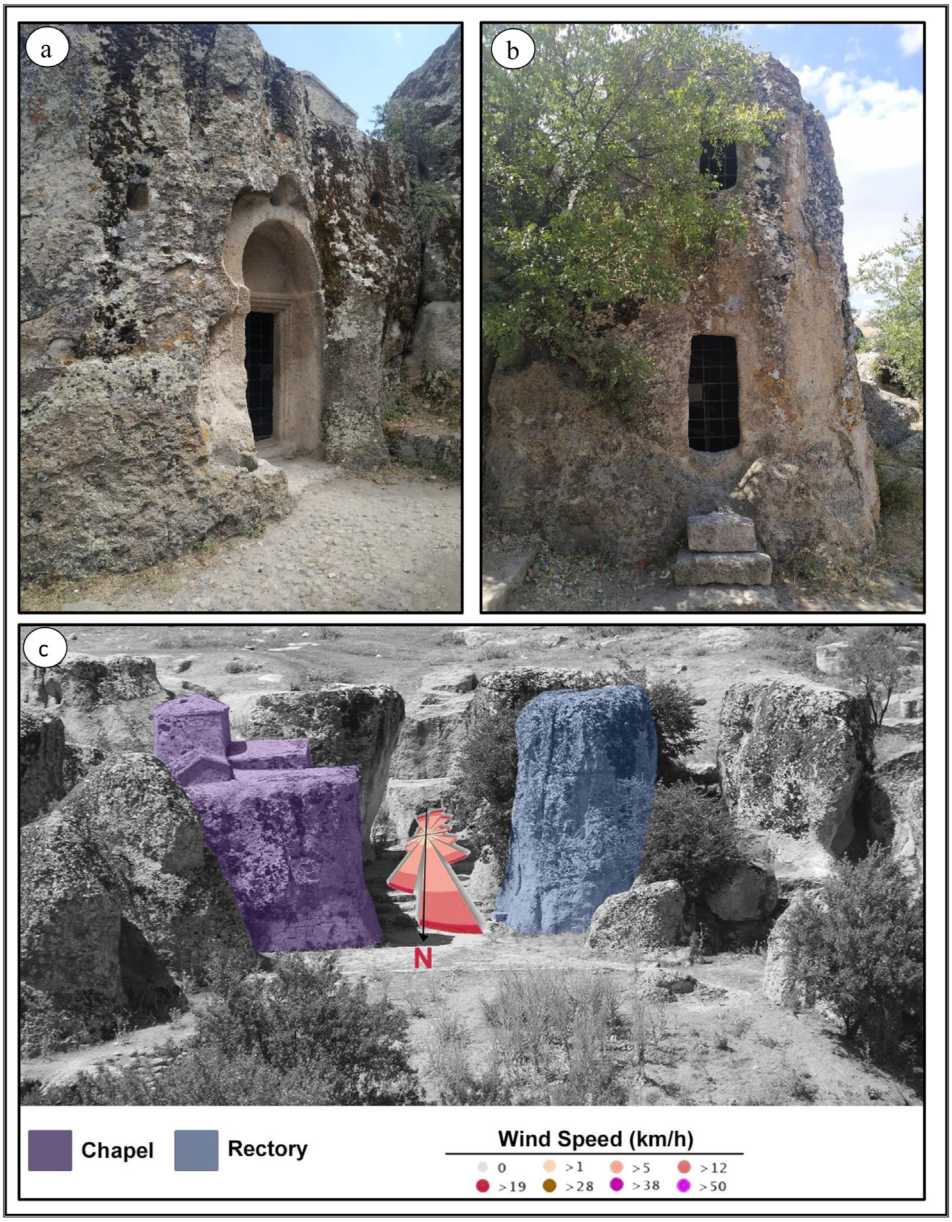

Fig. 2 Monuments examined in the ancient city of Kilistra: a) general view of the chapel, b) general view of the rectory c) location of the rectory and chapel and wind directions in the area.

the tests repeated five times was taken while determining the UCS value of the rock. The SHR test was performed to determine the change in the rock surface where the monument was carved. The hardness of the rock was determined *in situ* and in the laboratory by using an L-type Schmidt hammer. SHR test was performed in dry and saturated conditions according to the standard method recommended in ASTM D5873 (2014). While measuring, the Schmidt hammer was held in a horizontal position at right angles to the vertical monument surface. To determine the average number of SHR, 10 measurements were made at each designated point in the monument. The rebound values showing a deviation of seven units from the mean values were not included in the assessment. Then, SHR value was determined by re-averaging the remaining numbers.

To determine the petrographic properties of the rock used in the study, thin sections were prepared according to the method recommended in TS EN-12407 (2019), the samples were examined using a polarizing microscope, and definitions were made.

In situ NDT tests (SHR test, relative humidity, and P-wave velocity) were performed in two periods, summer and winter. Before starting non-destructive test studies, high-resolution photographs of the structures were taken from different angles, and orthophotos of each ancient structure were prepared using the Agisoft PhotoScan program. Then, since the structures were built by carving into the massive rock, temporary measurement points (grids) were created on the facades of the works so that the NDT measurement points would remain constant (Fig. 3). These photographs and grid points were used as a basis in later studies.

Table 2 Structural parts of the monuments studied.

Chapel		Rectory	
Picture	Description	Picture	Description
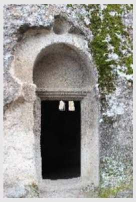	Entrance door		Entrance door
	Southern cross arm		Entrance floor
	Southern façade abscissa and altar		Passages between the floors
	Northern cross arm	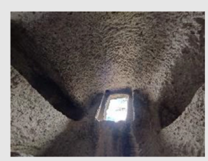	Second floor (bedroom); rock-carved beds and window
	Northern façade abscissa		
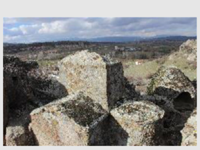	Roof of the chapel		

The surface hardness at the grid points on the facades of the selected monuments was determined using the ELE brand Schmidt hammer. Trotec T660, UK1401 ultrasonic brand devices were used, respectively, in the relative humidity and P-wave velocity measurements at the grid points. The Trotec T660 is a device that detects the moisture distribution near the surface (approximately 4 cm) using the dielectric method. The values of the *in situ*

Table 3 Meteorological data for Konya in the period 1929–2021 (MGM 2022).

Months	Minimum temperature (°C)	Maximum temperature (°C)	Average temperature (°C)	Monthly total precipitation (mm)	Average Sunbathing Time (hours)
January	4.2	4.6	−0.2	38.1	3.3
February	−3.3	7.0	1.5	28.5	4.6
March	−0.2	11.8	5.6	29.3	5.9
April	4.3	17.5	11.1	32.0	7.2
May	8.6	22.4	15.9	43.1	9.0
June	12.6	26.7	20.1	26.1	10.7
July	15.9	30.2	23.5	7.5	11.8
August	15.6	30.2	23.3	6.4	11.4
September	11.0	26.0	18.8	13.5	9.7
October	5.9	20.0	12.8	29.5	7.3
November	0.8	13.0	6.5	32.2	5.3
December	−2.3	6.6	1.7	43.2	3.2

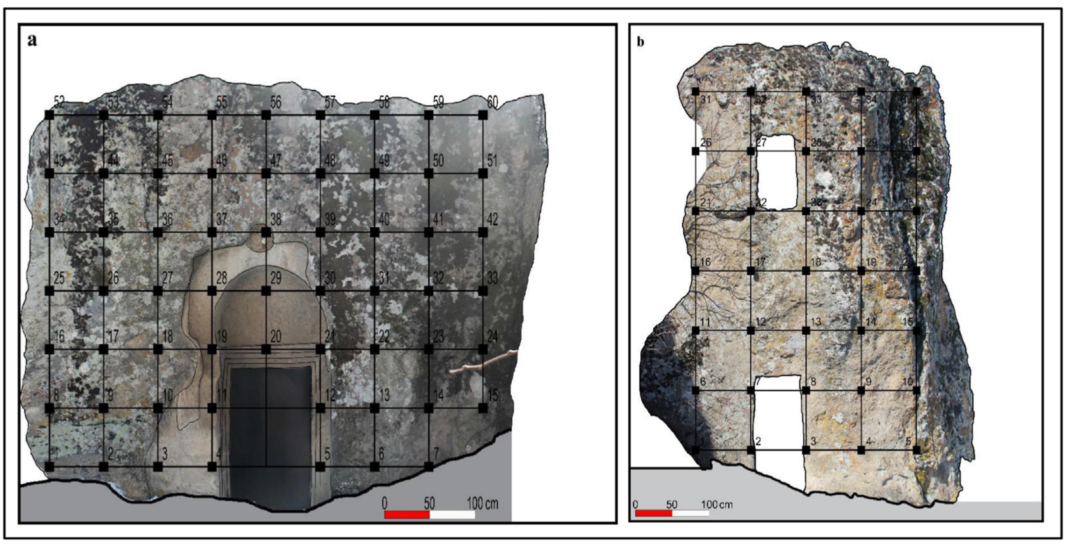

Fig. 3 Grid points in the monuments examined in the ancient city of Kilistra: a) Chapel, b) Rectory.

relative humidity and P-wave velocity measurements were calculated by taking the average of the measurements obtained by three different readings from the same point with the devices placed perpendicular to the building surface. With the NDT values measured in ancient buildings in the summer and winter periods, relative humidity, SHR, and P-wave velocity maps were created using the Surfer 17 program.

5. Results and discussion

5.1. Geological and petrographic properties

Gökyurt neighborhood and its surroundings, where the unit in which the ancient city of Kilistra was carved outcropped, was determined as the study area. Pre-Neogene units formed the basis of the study area. Neogene aged fluvial and lacustrine deposits overlie the basement with angular unconformity. Pyroclastic rocks overlie this unit with a lateral vertical transition. Temel et al. (1998) stated that pyroclastic rocks can be divided into subunits according to some properties (e.g., eruption, transport, deposition and welding). These units are cut by Neogene lava domes.

The ancient city of Kilistra was formed by carving the pyroclastic rocks. This unit was first named Erenkaya ignimbrite in the study conducted by Keller et al. (1977). The unit generally consists of gray and light gray tuff and ignimbrite levels. The unit is Late Miocene - Early Pliocene in age (Eren, 1993). In their study, Bozdağ et al. (2016) examined this unit in two subsections, lower pyroclastic unit (unwelded) and upper pyroclastic unit (welded). The ancient structures examined in this study are the structures carved in the upper pyroclastic unit (UPU). The UPU is gray-light gray in color and generally medium to locally fine-grained (Fig. 4a). In macro observations, pumice grains, plagioclase, pyroxene, amphibole and biotite phenol crystals and rock fragments are evident in the rock. Pumices are black and in the form of lenticular grains, about 1–5 cm long, elongated in one direction. These pumices gave the rock a fiamme structure (Fig. 4a).

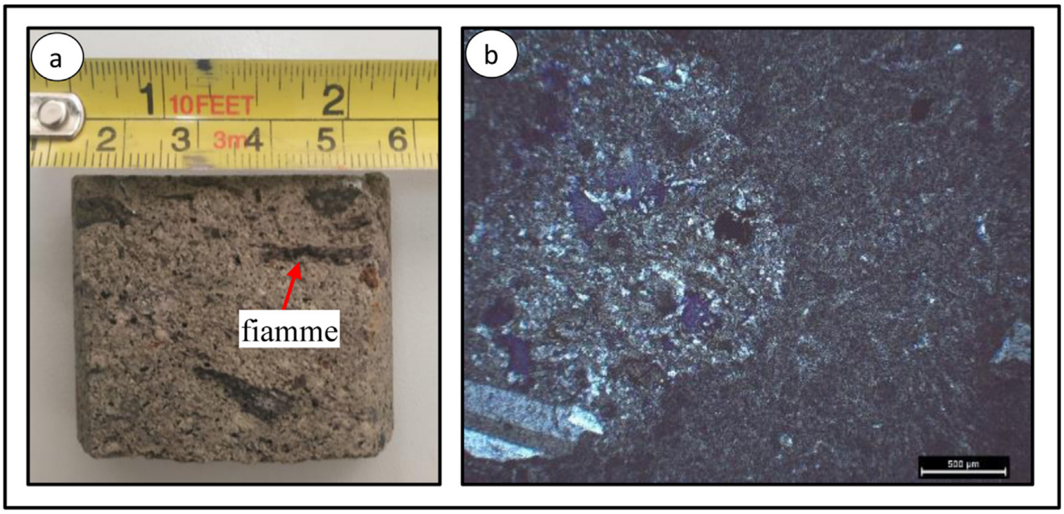

Fig. 4 Upper pyroclastic unit view of the Erenkaya ignimbrite: a) macroscopic image, b) polarizing microscope image (crossed polars).

Volcanic glass (67%), plagioclase (16%), rock fragment (11%), pyroxene (5%), and biotite (1%) were found in their mineralogical compositions (Fig. 4b). Considering the mineralogical composition and grain size of the rock, the rock was named "andesitic ignimbrite". The rock is vitric tuff according to the classification proposed by Schmid (1981). The rock has hyaline porphyritic texture features.

5.2. Physical-mechanical properties

The physical (porosity, dry density, capillary water absorption coefficient, and P-wave velocity) and strength (UCS and SHR) values of the rock from which the monuments were built are presented in Table 4. While the dry density of the rock was 1.75 g/cm^3, its porosity was 27.50%.

While the rock is included in the very high class according to the porosity classification of NBG (1985), it is included in the very low class according to the dry density classification of NBG (1985). The capillary water absorption value of the rock was determined as 156.85 $g/(m^2 \cdot s^{1/2})$. According to Snethlage (2005), it is included in the high water-absorbing rock class. The UCS value of the rock was determined as 14.50 MPa. The SHR values for the dry and saturated state of the rock were 36 and 33, respectively. While the P-wave velocity was 2.70 km/s for the dry state of the rock, the P-wave velocity is 2.57 km/s for the saturated state.

5.3. Deteriorations observed in the Kilistra ancient city

The types of deteriorations observed in the structures of the ancient city of Kilistra were named according to the definitions proposed in the ICOMOS-ISCS (2008). Contour scaling, crack, efflorescence and lichen, moss and higher plant formations, which are products of biological activity, were observed in different parts of the structures (Fig. 5). The cracks observed in the monuments were examined in two categories. The first ones were those associated with the geological elements in the region (Fig. 5a), and the other ones were those developed as a result of the structural problems that occurred in the monuments over time (Fig. 5b). In relation to climatic processes, the separation of the monument into scales varying from millimeters to centimeters on the outer surface was described as contour scaling (Fig. 5c). Efflorescence occurred widely in the capillary zones of the monuments examined (Fig. 5d). Efflorescence usually appears whitish, powdery, or crystalline on the rock surface and is usually poorly cohesive (Fig. 5d). Alga, lichen, and moss were commonly observed in the monuments (Fig. 5e). Furthermore, there were higher plant developments in the cracks observed in the structure (Fig. 5f).

5.4. Non-destructive test results

The sensitivity of the rocks to atmospheric processes increases as their degree of saturation increases (Chen et al., 2004). The determination of the presence of water is the most important factor in shedding light on the deterioration process in monuments built on rocks (Bozdağ et al., 2020; Hatır et al., 2019; İnce et al., 2018). In homogeneous monuments, important information can be obtained by using relative humidity meters in determining the distribution of water along a facade or surface (Orr et al., 2020). In this study, the change of water on the facades of both

Table 4 Physical and mechanical properties of the samples.

ρ_d (g/cm^3)	n (%)	*C* ($g/(m^2 \cdot s^{1/2})$)	*V*p-dry (km/s)	*V*p-saturated (km/s)	SHR-dry	SHR-saturated	UCS (MPa)
1.75	27.50	156.85	2.70	2.57	36.00	33.00	14.50

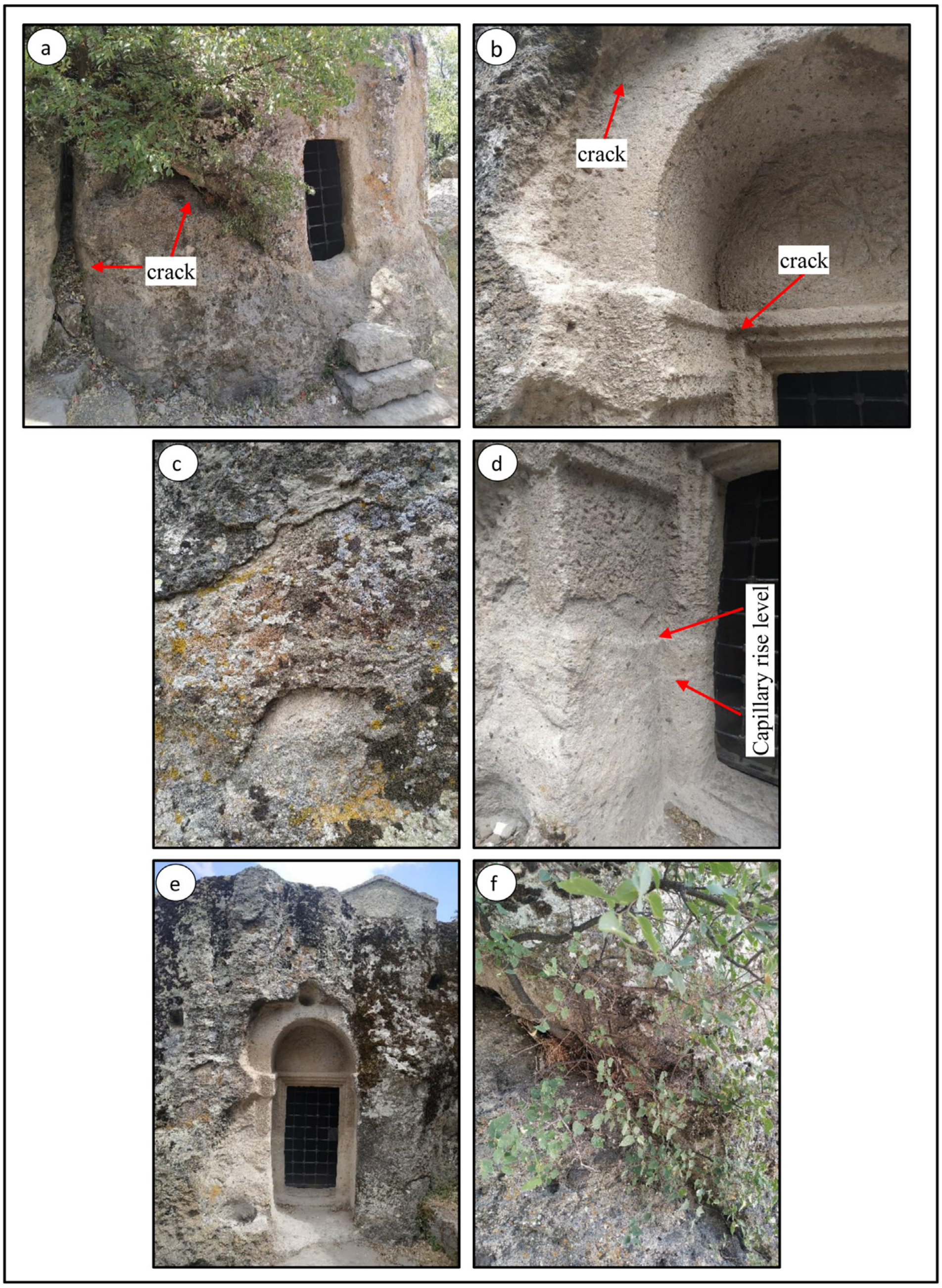

Fig. 5 Deteriorations observed in the monuments of the Kilistra ancient city: a-b) crack, c) contour scaling, d) efflorescence, e) lichen-moss, f) higher plant.

monuments in the summer and winter seasons was examined using relative humidity measurements, and surface moisture change maps were created using the data obtained (Figs. 6 and 7).

While the relative humidity values in the chapel varied between 54% and 84% for the winter period, these values were between 13% and 65% for the summer period. While the relative humidity values were high around the capillary zone and the discontinuity to the right of the monument in the measurement of the monument in the summer period, the relative humidity values were high in the infiltration zone in addition to these regions in the winter period. In the winter period, it was determined that the relative humidity values in the infiltration zone of the chapel decreased from the ceiling to the base of the monument. However, the relative humidity values in the capillary rise zone decreased from the ground level of the building to the upper levels (Fig. 6a). It caused the formation of a drier region in the central part of the monument compared to the other parts. The high capillary water absorption value of the rock facilitates the movement of water within the monument, which accelerates the deterioration time of the rock. While the water content in the monument causes the freeze–thaw (F–T) process in the rock to be effective in the winter period, it causes the salt crystallization (SC) process to be effective in the summer period. As a result of

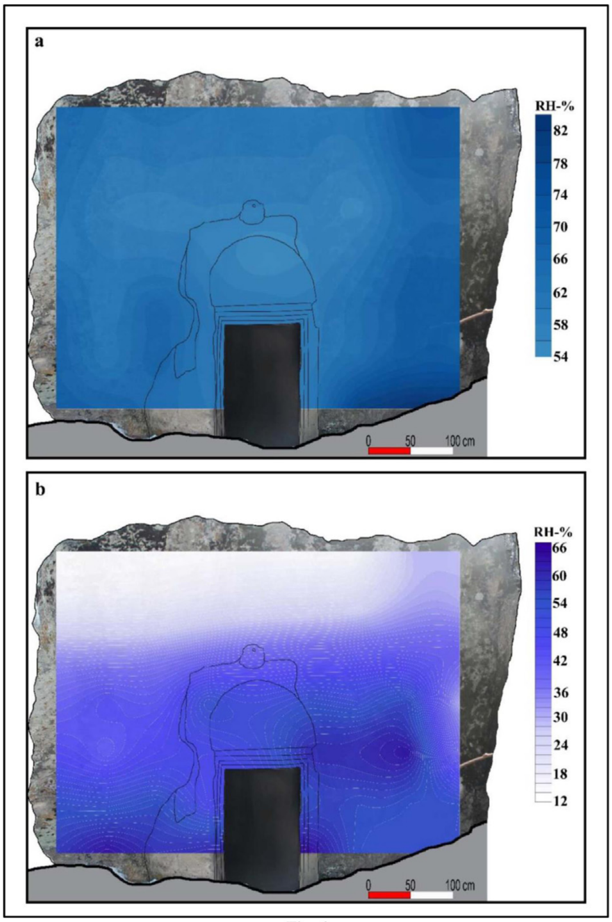

Fig. 6 Relative humidity map of the chapel: a) winter period, b) summer period.

the active deterioration in the monument in both periods, the capillary rise levels of the rock varied as the capillarity value of the rock increased (Fig. 5d).

While the relative humidity values in the rectory were found to be between 32% and 69% in the winter period, they were measured between 12% and 24% in the summer period (Fig. 7). When the relative humidity maps in the monument for the summer and winter periods were examined, it was observed that the humidity in the monument was associated with the capillary zone and also affected by the cracks and the door, which is the building element. In both measurement periods, it was determined that the door gap in the monument affected the capillary water rise, and consequently, there was a decrease in relative humidity contours above the door. Furthermore, increased relative humidity on the surface was observed along the lines of the cracks that cut the monument. The location of the monuments and the direct relationship between this location and sun exposure resulted in summer and winter relative humidity values that differed between the two buildings. The amount of water that penetrates structures, as well as fluctuations in climate and temperature, induce millimeter (e.g., flaking type deterioration)—to meter (e.g., contour scaling type deterioration)—sized deteriorations on the outside surfaces of monuments. These deteriorations alter the surface hardness of the monument's construction material. SHR is the most popular surface hardness measuring test used to determine these modifications (Aoki and Matsukura, 2007). Moreover, this is the method most frequently employed to empirically calculate the rock's UCS value (Aydin and Basu, 2005). Summer and winter SHR measurements were done to determine the surface hardness change of the monuments under investigation. The maps prepared using the summer and winter SHR values of the examined monuments are presented in Figs. 8 and 9. While the SHR values measured in the monument in the winter period varied between 12 and 28, the SHR values measured for the summer period were between 16 and 30. When the SHR measurements of both monuments in the summer and winter periods were examined, it was determined that the low values were in the capillary zone. Furthermore, low SHR values were measured

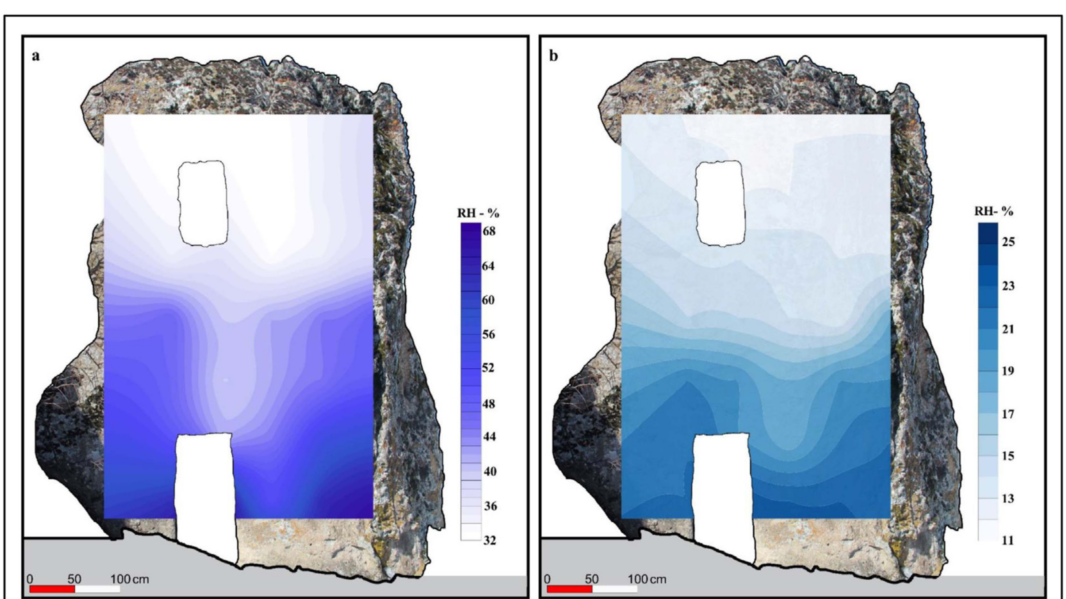

Fig. 7 Relative humidity map of the rectory: a) winter period, b) summer period.

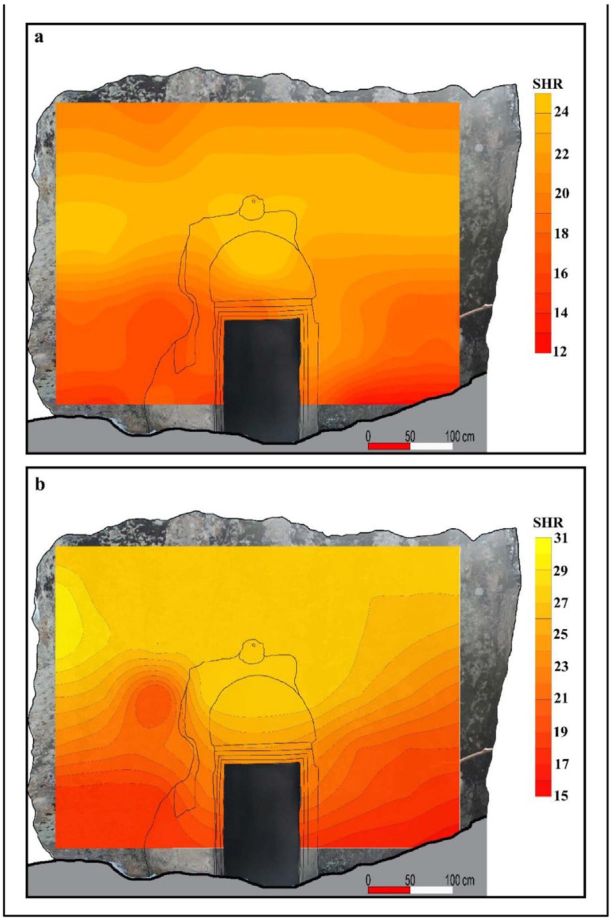

Fig. 8 SHR map of the chapel: a) winter period, b) summer period.

in the crack line zone in the rectory. When the SHR maps for the summer and winter periods were examined, it was determined that there was a 3—5 unit difference between the SHR values, which was considered to be due to the water content of the rock in the measurement periods. This is consistent with the difference between the dry and saturated SHR measurements of this fresh rock. P-wave velocity is a commonly used test for modeling atmospheric processes in the laboratory environment of building blocks due to its ability to identify changes in the internal structure of rocks (discontinuity development, increase in porosity) (Gokçe et al., 2016; Guler et al., 2021; Yavuz, 2011). This is the preferred NDT technique for assessing the deterioration of monuments directly exposed to atmospheric processes and detecting structural faults (Bozdağ et al., 2020; Hatır, 2020; İnce et al., 2018). For this reason, P-wave velocity measurements were made on the facade of both monuments. While P-wave velocity values for the facades of the monuments in the summer period varied between 1.10 km/s and 2.22 km/s, no measurement could be performed on the facades of the monuments in the winter period (Fig. 10). Low P-wave velocity values in the monuments were associated with capillary, infiltration, and crack zones. It was observed that the P-wave velocity maps of the monuments were compatible with the maps prepared from other NDTs. With the effects of the atmospheric process in the rock in which the monuments were carved, significant decreases were observed in SHR values (16—30) compared to the SHR value of fresh rock (36). There was also a similar decrease for the P-wave velocity values. As previously indicated by experts, SHR (Aydın, 2014; Karakul, 2017; Sumner and Nel, 2002) and P-wave velocity (Kahraman et al., 2017; Karakul and Ulusay, 2013) values are closely related to the rock's moisture content. Aydın (2014) said that the moisture content of the rock inside the impact region of the SHR test will greatly reduce the SHR values, but Kahraman et al. (2017) stated that the moisture content will decrease the P-wave velocity in rocks with a porosity of more than 20%. If the SHR and P-wave velocity values acquired during the winter season, when the rock's moisture content increases, are directly correlated with the rock's weathering process and

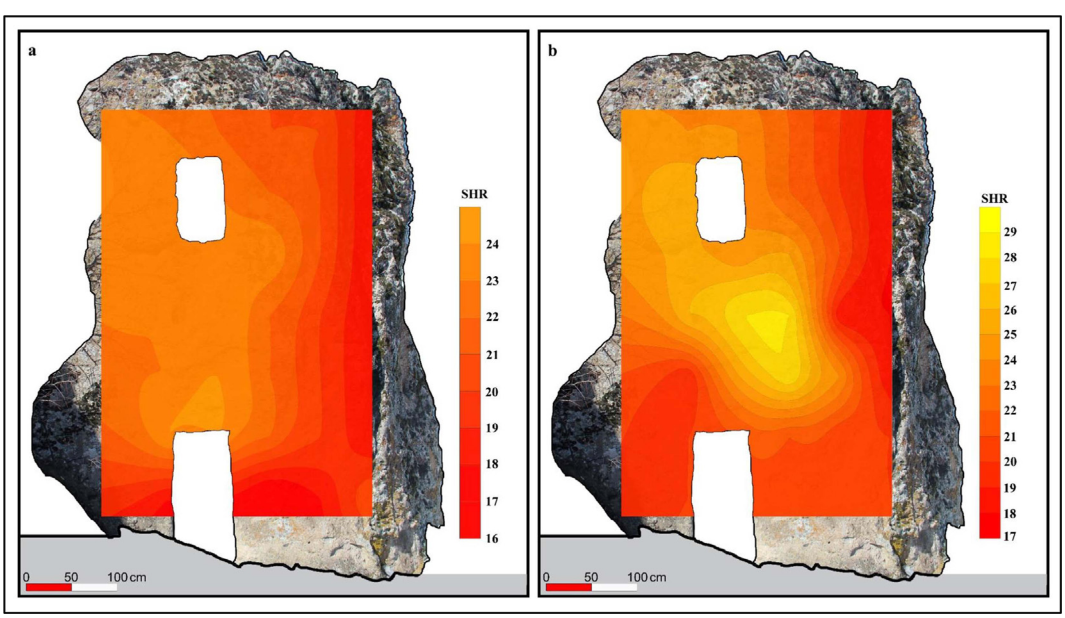

Fig. 9 SHR map of the rectory: a) winter period, b) summer period.

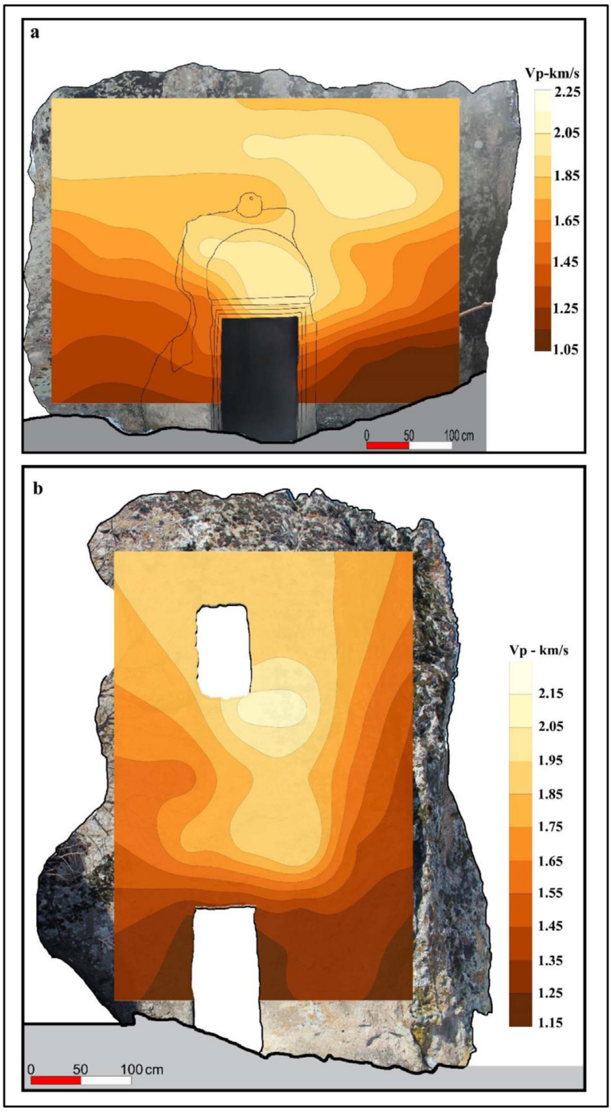

Fig. 10 Summer *V*p map: a) Chapel, b) Rectory.

accepted as data for restoration efforts, the results may be inaccurate. It is believed that taking SHR and P-wave velocity measurements in the summer, when the rocks are drier, is better suitable for this purpose, and that these data can be applied to restoration studies. In the relative humidity maps of the summer and winter periods in the monuments, drier regions were determined between the capillary, infiltration, and crack zones. In other NDT maps, it was determined that the rock properties were better in these regions, which revealed the importance of reducing water intrusion into the monument to protect the monuments built on low-strength rocks.

5.5. Discussion

Numerous researchers in the laboratory have modeled the climate characteristics of the region, the mineralogical composition of the rock, and changes in the textural and index-strength properties to better comprehend the deterioration process of the building blocks on which the monuments are constructed (Fener and İnce, 2015; Guler et al., 2021; Huang et al., 2022; Liu et al., 2018; Özşen et al., 2017). In order to simulate natural atmospheric processes, accelerated weathering experiments (wetting-drying, freeze-thaw, thermal shock, and salt crystallization) were utilized in these research. In these weathering tests, the changes in the rock's textural (Fener and İnce, 2015; Liu et al., 2018; Özşen et al., 2017), index (Gökçe et al., 2016; Wang et al., 2019), and strength properties (Guler et al., 2021; Huang et al., 2022; Yahaghi et al., 2022) were studied. They asserted that following the F−T (Fener and İnce, 2015) and SC (Özşen et al., 2017) processes, new fractures formed in the phenocrystals of the rock's microtexture, while the pore ratio rose in the paste phase. According to certain researchers (Gökçe et al., 2016; Wang et al., 2019), while accelerated deterioration tests enhanced the porosity of the rock, the P-wave velocity decreased. İnce and Fener (2016), Guler et al. (2021), and Xiong et al. (2022) noted that when rocks are subjected to fast weathering, their strength values fall. Although laboratory-created models do not perfectly represent the natural environment, they do provide some helpful information. To this end, investigations were done in which NDT were used to determine and explain the observed deterioration of structures *in situ* (Korkanç et al., 2018, 2021; İnce et al., 2020; Zhang et al., 2019). Using on-site NDT, previous research analyzed the change in the index-reducing qualities of the monument's building blocks as a result of atmospheric processes and developed change maps based on this data. Bozdag et al. (2016) investigated the change in the rock properties of the ancient city of Kilistra using wetting-drying, F−T and SC from accelerated weathering experiments carried out in the laboratory. In this study, the deteriorations in the UPU carved structures in the ancient city of Kilistra were investigated by NDT methods. According to Bozdağ et al. (2016), the porosity values of the samples in accelerated deterioration tests increased following the F−T and SC processes, whereas the UCS values fell in the rock unit (UPU) where the structures were constructed. The maps generated from *in situ* SHR measurements to assess strength value are consistent with the reduction in rock strength value caused by weathering. The maps generated from the P-wave velocity values, which are inversely related to the porosity values of the rocks, are consistent with alexperimental data Baozdağ et al. (2016). As a result of the 10th cycle of accelerated deterirations tests (F−T and SC), crack development was observed in the samples (Bozdağ et al., 2016). In this study, the crack development observed in the field at the macro scale can be attributed to atmospheric processes. However, based on field observations, it was determined that the continuity of the cracks in Fig. 5a was due to geological factors, whereas the crack in Fig. 5b was due to structural loads. In addition, cracks and capillary zones where high humidity is determined in buildings are the regions where possible problems will intensify in the future. Similar problems in cultural structures have been investigated *in situ* by some researchers in laboratories or masonry walls (Monczynski et al., 2019; Sardella et al., 2018; Silva et al., 2014). In these studies, grouting was applied to the cavities to reduce cracks or porosity. This application also reduced the porosity of the structure and the capillary movement of water in the rock. There are no examples of this application in the structures created by carving the rock. In addition, the negative effects of the application are not known. Although the damage caused by water and discontinuities and atmospheric processes may be observed on the facades of monuments, the relevance of biodeterioration of lichen, moss, and high formation plants, which are products of living activity, should not be overlooked. The places where moisture is concentrated in moisture maps are conducive to the growth of biological colonization. It is recommended to monitor the development of biological colonization in structures.

Considering these data, although the experimental data obtained in the laboratory are very important, they do not completely reflect the deterioration caused by nature in the structures. This emphasizes the significance of *in situ* NDT in the study of deterioration processes. In addition, NDT will increase the popularity of this method in restoration applications due to its non-destructive feature and easy applicability in determining the deterioration status of cultural monuments where sampling is limited or impossible. In addition to these features, providing information about the monument's surface and interior structure may pave the way for NDT applications to be used in restoration applications in the future. It will aid in determining the origin of deterioration processes as well as the locations where deterioration condenses, particularly in cultural heritage formed by carving into weak-strength rocks. It is anticipated that these methods will greatly assist restorers in monitoring the success of the improvements made to the monuments.

6. Conclusions

Cultural monuments built from low-strength rocks around the world are susceptible to atmospheric processes. Based on the size and intensity of the deteriorations, it is also crucial to take necessary steps for restorations and rehabilitation works. In this study, the results obtained from the visual inspection and *in situ* NDT measurements made in two structures built in low-strength rocks in the ancient city of Kilistra are given below.

- The monuments examined were built by carving into the upper pyroclastic unit, which represents the welded level of the Late Miocene–Early Pliocene pyroclastic rock. The unit is gray to light gray in color and generally medium to fine grained. Phenocrysts (plagioclase, pyroxene, amphibole and biotite), pumice grains and rock fragments in the rock can be identified with the naked eye. Considering the mineralogical composition-grain size of the rock, it is "andesitic ignimbrite" and shows a hyaline porphyritic texture.
- The dry density, porosity and UCS values of the rock were determined as 1.75 g/cm^3, 27.50% and 14.50 MPa, respectively. While the low strength and high porosity of the rocks facilitated the construction of the monument, these features increased the sensitivity of the structure to atmospheric processes. In addition to this, the fact that the capillary water absorption value of the building material is in the high water absorbing rock class (*C*: 156.85 $g/(m^2 \cdot s^{1/2})$) increased the mobility of water in the monument and accelerated the deterioration process.
- Contour scaling, crack, efflorescence and biological colonization (alga, lichen, moss and higher plant) type deteriorations were detected in the monuments.
- The highest moisture content values on the chapel facade in the summer and the winter periods are 65% and 84%, respectively. While the relative humidity value on the facade of the Rectory was 24% for the summer period, this value was determined as 69% in the winter period measurements. While the water content in the monument was explained by the capillary rise of the water in the summer, it was associated with the effect of capillary and infiltration water in the winter. The high moisture content on the facades of the buildings has increased the contour scaling, efflorescence and biological colonization (alga, lichen, and moss) type deterioration.
- The discontinuities limiting the monuments help the transfer of capillary water to higher levels and increase moisture values in crack-related regions. In addition, the presence of water in these regions has intensified the formation of biological colonization.
- Moisture content increased in the chapel (minimum value increase: 41%) and rectory (minimum value increase: 30%) facades during the winter period. As a result of the increase in the moisture value of the rock in the winter period, the SHR values measured (3—4 unit) on the facade of the monument decreased. This indicated that it is crucial to determine the periodic change of water distribution in the monuments. Since NDT (SHR and *V*p) measurements are directly affected by the presence of water in rocks, it is more useful to make these measurements during the dry season. In addition, it is recommended to take the necessary measures to prevent the damages that may be caused by the high water content in the monuments during the winter periods.
- With the effect of the repeated atmospheric processes to which monuments were exposed, the SHR (the minimum measured value is 16) and *V*p (minimum measured value, 1.10 km/s) values of the rock forming the structure significantly decreased compared to the SHR (33) and *V*p (2.70 km/s) values of the fresh rock. It is recommended to monitor the deterioration processes in these monuments with regular NDT (SHR and *V*p) measurements. Thus, damages that may occur in the monuments are prevented before they increase.

Water content accelerates atmospheric processes in cultural monuments built by low-strength rock. This situation increases the importance of regularly controlling the change of water content in buildings. *In situ* NDT measurements are a very practical method for determining the index and strength properties of building stones. These data will help to prevent damages in cultural heritages and therefore to transfer these structures to the future generations. In addition, simulation studies at a regional scale should be planned and applied to determine the effects of climate changes on the degradation process in such structures.

Declaration of competing interest

The authors declare that they have no known competing financial interests or personal relationships that could have appeared to influence the work reported in this paper.

Acknowledgments

This research was supported by the grants from Scientific Research Foundation of Adıyaman University MÜFYL/2017-0001. Two anonymous referees are gratefully acknowledged for their helpful suggestions and constructive comments on the manuscript.

References

Aoki, H., Matsukura, Y., 2007. A new technique for non-destructive field measurement of rock-surface strength: an application of the Equotip hardness tester to weathering studies. Earth Surf. Process. Landforms: J British Geomorphologic Res. Group 32 (12), 1759—1769.

ASTM D5873, 2014. Standard Test Method for Determination of Rock Hardness by Rebound Hammer Method. ASTM International, West Conshohocken.

ASTM E494, 2010. Standard Practice for Measuring Ultrasonic Velocity in Materials. ASTM International, West Conshohocken.

Aydın, A., 2014. ISRM suggested method for determination of the Schmidt hammer rebound hardness: revised version. In: Ulusay, R. (Ed.), The ISRM Suggested Methods for Rock Characterization, Testing and Monitoring: 2006—2014. Springer, Heidelberg, pp. 1—22.

Aydin, A., Basu, A., 2005. The Schmidt Hammer in rock material characterization. Eng. Geol. 81, 1—14.

Bozdağ, A., 2022. Rockfall hazard assessment in a natural and historical site: the case of ancient Kilistra settlement (Konya), Turkey. J. Mountain Sci. 19 (1), 151—166.

Bozdağ, A., Bayram, A.F., İnce, İ., Asan, K., 2016. The relationship between weathering and welding degree of pyroclastic rocks in the Kilistra ancient city, Konya (Central Anatolia, Turkey). J. Afr. Earth Sci. 123, 1—9.

Bozdağ, A., İnce, İ., Bozdağ, A., Hatır, M.E., Tosunlar, M.B., Korkanç, M., 2020. An assessment of deterioration in cultural heritage: the unique case of Eflatunpınar Hittite Water Monument in Konya, Turkey. Bull. Eng. Geol. Environ. 79, 1185—1197.

Chen, T.C., Yeung, M.R., Mori, N., 2004. Effect of water saturation on deterioration of welded tuff due to freeze-thaw action. Cold Reg. Sci. Technol. 38, 127—136.

Christaras, B., 1997. Estimation of damage at the surface of stones using non destructive techniques. WIT Trans. Built Environ. 26, 121—128.

Christaras, B., Cuccuru, F., Fais, S., Papanikolaou, H., 2015. Application of non destructive ultrasonic techniques for the analysis of the conservation status of building materials in monumental structures. In: Lollino, G., Giordan, D., Marunteanu, C., Christaras, B., Yoshinori, I., Margottini, C. (Eds.), Engineering Geology for Society and Territory, vol. 8. Springer, Cham, pp. 139—143.

TS EN-12407, 2019. Natural Stones-Test Methods-Petrographical Investigation. Turkish Standards Institution, Ankara (in Turkish).

TS EN-1925, 2000. Natural Stone Test Methods Determination of Water Absorption Coefficient by Capillarity. Turkish Standards Institution, Ankara (in Turkish).

Eren, Y., 1993. The Geology of the Eldeş-Derbent-Tepeköy-Söğütözü (Konya) Region. PhD. Thesis. Selçuk University (in Turksh).

Fais, S., Cuccuru, F., Ligas, P., Casula, G., Bianchi, M.G., 2017. Integrated ultrasonic, laser scanning and petrographical characterisation of carbonate building materials on an architectural structure of a historic building. Bull. Eng. Geol. Environ. 76, 71—84.

Fener, M., İnce, İ., 2015. Effects of the freeze—thaw (F—T) cycle on the andesitic rocks (Sille-Konya/Turkey) used in construction building. J. Afr. Earth Sci. 109, 96—106.

Fookes, P.G., Dearman, W.R., Franklin, J.A., 1971. Some engineering aspects of rock weathering with field examples from Dartmoor and elsewhere. Q. J. Eng. Geol. Hydrogeol. 4, 139—185.

Fort, R., Alvarez de Buergo, M., Perez-Monserrat, E.M., 2013. Non-destructive testing for the assessment of granite decay in heritage structures compared to quarry stone. Int. J. Rock Mech. Min. Sci. 61, 296—305.

Gökçe, M.V., Ince, I., Fener, M., Taşkıran, T., Kayabali, K., 2016. The effects of freeze—thaw (F—T) cycles on the Gödene travertine used in historical structures in Konya (Turkey). Cold Reg. Sci. Technol. 127, 65—75.

Guler, S., Türkmenoğlu, Z.F., Varol, O.O., 2021. Thermal shock and freeze-thaw resistance of different types of carbonate rocks. Int. J. Rock Mech. Min. Sci. 137, 104545.

Hatır, M.E., 2020. Determining the weathering classification of stone cultural heritage via the analytic hierarchy process and fuzzy inference system. J. Cult. Herit. 44, 120—134.

Hatır, M.E., Korkanç, M., Başar, M.E., 2019. Evaluating the deterioration effects of building stones using NDT: the Küçükköy Church, Cappadocia Region, central Turkey. Bull. Eng. Geol. Environ. 78, 3465—3478.

Hatır, M.E., İnce, İ., Bozkurt, F., 2022. Investigation of the effect of microclimatic environment in historical buildings via infrared thermography. J. Build. Eng. 57, 104916.

Huang, S., He, Y., Yu, S., Cai, C., 2022. Experimental investigation and prediction model for UCS loss of unsaturated sandstones under freeze-thaw action. Int. J. Min. Sci. Technol. 32 (1), 41—49.

ICOMOS-ISCS, 2008. International council on monument and sites international scientific committee for stone, Illustrated glossary on stone deterioration patterns. In: Ateliers 30 Impresión. Champigny/Marne, France.

İnce, İ., Fener, M., 2016. A prediction model for uniaxial compressive strength of deteriorated pyroclastic rocks due to freeze—thaw cycle. J. Afr. Earth Sci. 120, 134—140.

İnce, İ., Bozdağ, A., Tosunlar, M.B., Hatır, M.E., Korkanç, M., 2018. Determination of deterioration of the main facade of the Ferit Paşa Cistern by non-destructive techniques (Konya, Turkey). Environ. Earth Sci. 77, 420.

İnce, İ., Korkanç, M., Hatır, M.E., 2020. Evaluatıon of weatherıng effects due to surface and deep moisture in a roman rock tomb: lukianos monument Konya (Turkey). Mediterr. Archaeol. Archaeometry. 20, 121—133.

ISRM, 2007. The Complete ISRM suggested methods for rock characterization, testing and monitoring: 1974—2006. In: Ulusay, R., Hudson, J. (Eds.), Suggested Methods Prepared by the Commission on Testing Methods. ISRM Turkish National Group, Ankara, Turkey.

Jo, Y.H., Lee, C.H., 2014. Quantitative modeling and mapping of blistering zone of the Magoksa Temple stone pagoda (13th century, Republic of Korea) by graduated heating thermography. Infrared Phys. Technol. 65, 43—50.

Kahraman, S., Fener, M., Kilic, C.O., 2017. Estimating the wet-rock P-wave velocity from the dry-rock P-wave velocity for pyroclastic rocks. Pure Appl. Geophys. 174 (7), 2621—2629.

Karakul, H., 2017. Investigation of saturation effect on the relationship between compressive strength and Schmidt hammer rebound. Bull. Eng. Geol. Environ. 76 (3), 1143—1152.

Karakul, H., Ulusay, R., 2013. Empirical correlations for predicting strength properties of rocks from P-wave velocity under different degrees of saturation. Rock Mech. Rock Eng. 46 (5), 981—999.

Keller, J., Jung, D., Burgath, K., Wolff, F., 1977. Geologie und petrologie des Neogenen kalkalkali-vulkanismus von Konya Erenler Dağı - alacadağ Massiv. Zentral-Anatolien. Geol. Jb. B25, 37—117.

Kilic, G., 2015. Using advanced NDT for historic buildings: towards an integrated multidisciplinary health assessment strategy. J. Cult. Herit. 16, 526—535.

Korkanç, M., İnce, İ., Hatır, M.E., Tosunlar, M.B., 2018. Historical granaries at Taşkale (Turkey) under risk: a geotechnical analysis. Mediterr. Archaeol. Archaeometry. 18 (1), 149—162.

Korkanç, M., Hüseyinca, M.Y., Hatır, M.E., Tosunlar, M.B., Bozdağ, A., Özen, L., İnce, İ., 2019. Interpreting sulfated crusts on natural building stones using sulfur contour maps and infrared thermography. Environ. Earth Sci. 78, 378.

Korkanç, M., İnce, İ., Hatır, M.E., Tosunlar, M.B., 2021. Atmospheric and anthropogenic deterioration of the İvriz rock monument: ereğli-Konya, Central Anatolia, Turkey. Bull. Eng. Geol. Environ. 80, 3053—3063.

Liu, C., Deng, H., Zhao, H., Zhang, J., 2018. Effects of freeze-thaw treatment on the dynamic tensile strength of granite using the Brazilian test. Cold Reg. Sci. Technol. 155, 327—332.

MGM (General Directorate of Meteorology), 2022. Available on the Website of Mam.gov.

Mimiroğlu, İ.M., 2005. Ortaçağ'da Konya-Kilistra kenti yapıları, Master Thesis. Selçuk University (in Turksh).

Mol, L., Preston, P.R., 2010. The writing's in the wall: a review of new preliminary applications of electrical resistivity tomography within archaeology. Archaeometry 52, 1079—1095.

Monczynski, B., Ksit, B., Szymczak-Graczyk, A., 2019. Assessment of the effectiveness of secondary horizontal insulation against rising damp performed by chemical injection. IOP Conf. Ser. Mater. Sci. Eng. 471 (5), 052063.

NBG, 1985. Engineering Geology and Rock Engineering. Norwegian Group of Rock Mechanics, Fornebu-Norway.

Orr, S.A., Fusade, L., Young, M., Stelfox, D., Leslie, A., Curran, J., Viles, H., 2020. Moisture monitoring of stone masonry: a comparison of microwave and radar on a granite wall and a sandstone tower. J. Cult. Herit. 41, 61—73.

Özkan, N., 2001. Konya-meram-gökyurt koyu Kilistra antik kenti kurtarma temizlik ve onarım çalışmaları (1998-1999). In: Olşen, K. (Ed.), 11. Müze Çalışmaları Ve Kurtarma Kazıları Sempozyumu 24-26 Nisan 2000 Denizli, Kültür Bakanlığı Milli Kütüphane Basımevi Ankara (in Turksh).

Özşen, H., Bozdağ, A., İnce, İ., 2017. Effect of salt crystallization on weathering of pyroclastic rocks from Cappadocia, Turkey. Arabian J. Geosci. 10 (12), 1—8.

Sardella, A., De Nuntiis, P., Rizzo, M., Giosuè, C., Tittarelli, F., Bonazza, A., 2018. In situ performance evaluation of chemical injections against rising damp: a case study in Italy. Measurement 130, 128—136.

Schmid, R., 1981. Descriptive nomenclature and classification of pyroclastic deposits and fragments: recommendations of the international union of geological sciences subcommission on the systematics of igneous rocks. Geol. 9, 41—43.

Silva, B., Dalla Benetta, M., da Porto, F., Valluzzi, M.R., 2014. Compression and sonic tests to assess effectiveness of grout injection on three-leaf stone masonry walls. Int. J. Architect. Herit. 8 (3), 408—435.

Snethlage, R., 2005. Leitfaden Steinkonservierung. Fraunhofer IRB Verlag, Stuttgart.

Sumner, P., Nel, W., 2002. The effect of rock moisture on Schmidt hammer rebound: tests on rock samples from Marion Island and South Africa. Earth Surf. Process. Landforms 27 (10), 1137—1142.

Temel, A., Gundogdu, M., Gourgaud, A., 1998. Petrological and geochemical characteristics of Cenozoic high-K calc-alkaline volcanism in Konya, Central Anatolia, Turkey. J. Volcanol. Geoth. Res. 85, 327—354.

Tosunlar, M.B., Hatır, M.E., İnce, İ., Bozdağ, A., Korkanç, M., 2018. The determination of deteriorations on the Mısırlıoğlu Bridge (Konya, Turkey) by non-destructive techniques (NDT). ICONARP Int. J. Archit. Plann. 6 (2), 399—412.

Tosunlar, M.B., Beycan, A.D.O., Korkanç, M., 2020. Non-destructıve test investigations on the deterioration of roman mausoleum in Karadağ central Anatolia, Turkey. Mediterranean Archaeol Archaeometry 20, 199—219.

Valero, L.R., Sasso, V.F., Vicioso, E.P., 2019. In situ assessment of superficial moisture condition in façades of historic building using non-destructive techniques. Case Stud. Constr. Mater. 10, e00228.

Wang, L., Li, N., Qi, J., Tian, Y., Xu, S., 2019. A study on the physical index change and triaxial compression test of intact hard rock subjected to freeze-thaw cycles. Cold Reg. Sci. Technol. 160, 39—47.

Wu, Y., Li, Q., Tong, H., He, Z., Qu, J., Zhang, B., 2021. Monitoring the deterioration of masonry relics at a UNESCO world heritage site. KSCE J. Civ. Eng. 25, 3097—3106.

Xiong, X., Gao, F., Zhou, K., Yang, C., Li, J., 2022. Mechanical properties and strength evolution model of sandstone subjected to freeze—thaw weathering process: considering the confining pressure effect. Mathematics 10 (20), 3841.

Yahaghi, J., Liu, H., Chan, A., Fukuda, D., 2022. Experimental, theoretical and numerical modelling of the deterioration and failure process of sandstones subject to freeze—thaw cycles. Eng. Fail. Anal. 141, 106686.

Yavuz, H., 2011. Effect of freeze—thaw and thermal shock weathering on the physical and mechanical properties of an andesite stone. Bull. Eng. Geol. Environ. 70 (2), 187—192.

Zhang, J., Huang, J., Liu, J., Jiang, S., Li, L., Shao, M., 2019. Surface weathering characteristics and degree of niche of Sakyamuni entering nirvana at Dazu rock carvings, China. Bull. Eng. Geol. Environ. 78, 3891—3899.